

Effect of Silica Fume on the Performances of Self-compacting Repair Mortar



Meriem Euldji¹, Mohamed Ghrici^{1,*}, Said Choucha¹ and Jamal Khatib²

¹Department of Civil Engineering, Hassiba Benbouali University of Chlef, P.O. Box c 78: Chlef 02180, Algeria

²Department of Civil Engineering, Beirut Arab University, Beirut, Lebanon

Abstract:

Background: Concrete is a widely utilized material in construction worldwide. However, concrete performance could be damaged under aggressive environments, therefore, many concrete structures may require repair and frequent maintenance.

Objective: The aim of this study is to develop reinforced Self-Consolidating Repair Mortars (SCRMs) incorporating silica fume and polypropylene fibers.

Methods: This research aimed to study the effect of silica fume as an alternative supplementary cementitious material (SCM) on the performance of fiber reinforced self-consolidating repair mortars (SCRMs). For this purpose, five SCRMs mixes incorporating 0%, 5%, 10%, 15%, and 20% of silica fume as partial cement replacement were prepared. Testing included slump flow, flow time, and unit weight, air-dry unit weight, compressive and flexural strengths, dynamic modulus of elasticity and water absorption.

Results: The results indicated that the substitution of cement by 15% of silica fume improves the flexural strength and slightly reduce the compressive strength of the fiber-reinforced repair mortar. The lowest values of total shrinkage, water capillary absorption, and sorptivity were observed for repair mortars containing 10% silica fume. In addition, bonding results between repair mortars containing silica fume and old concrete substrate investigated by the bond flexural strength test showed good interlocking, justifying the effectiveness of these produced mortars.

Conclusion: The results reveal that structural repair mortars containing 10 and 15% silica fume conform to the performance requirements of class R4 materials (European Standard EN 1504-3) and could be used in repair applications.

Keywords: Self-consolidating repair mortar (SCRM), Silica fume, Polypropylene fibers, Flowability, Mechanical properties, Bond flexural strength.

© 2024 The Author(s). Published by Bentham Open.

This is an open access article distributed under the terms of the Creative Commons Attribution 4.0 International Public License (CC-BY 4.0), a copy of which is available at: <https://creativecommons.org/licenses/by/4.0/legalcode>. This license permits unrestricted use, distribution, and reproduction in any medium, provided the original author and source are credited.

*Address correspondence to this author at the Department of Civil Engineering, Hassiba Benbouali University of Chlef, P.O. Box c 78: Chlef 02180, Algeria; E-mail: m_ghrici@yahoo.fr

Cite as: Euldji M, Ghrici M, Choucha S, Khatib J. Effect of Silica Fume on the Performances of Self-compacting Repair Mortar. Open Civ Eng J, 2024; 18: e18741495316659. <http://dx.doi.org/10.2174/0118741495316659240930054319>



Received: August 13, 2024

Revised: August 31, 2024

Accepted: September 10, 2024

Published: December 27, 2024



Send Orders for Reprints to reprints@benthamscience.net

1. INTRODUCTION

Concrete is a widely utilized material in construction worldwide. Unfortunately, the performance of concrete structures may show some degradation during their service life due to the materials used in the concrete mix

and the various exposure conditions [1]. Porosity is one of the properties affecting the durability of cementitious materials. The higher water absorption of porous aggregates leads to a higher penetration of aggressive agents, which significantly worsens the durability of

reinforced concrete structures [2, 3].

Other factors influencing the durability of concrete structures include mechanical loading, exposure to fire, extreme conditions, environmental pollution, and poor maintenance [4-6].

Finding appropriate materials with good performance and creating restoration technologies can lead to better durability but can be more challenging [7-9]. In a broader context, it is essential to possess technical expertise for evaluating the lifespan of a structure, as this facilitates the implementation of appropriate measures to ensure its optimal performance throughout its operational life. The speed of placement with adequate strength and improved durability characteristics suggest that self-compaction mortar (SCM) could be utilized as an alternative to conventional repair materials [10, 11].

Self-compacting mortar represents a significant advancement in high-performance mortars developed over the past forty years. One of its primary characteristics is its ability to spread and settle under its own gravity, thereby removing the need for vibratory compaction during application [12, 13]. This property not only simplifies the application process but also guarantees a uniform and high-quality finish, even in intricate formwork and areas with dense reinforcement. Additionally, this technique has the benefit of overcoming the shortage in the number of skilled workers for handling and applying mortar [14]. It has been suggested that appropriate volumes of water, cement, super-plasticizer, and just a small amount of coarse materials such as sand and gravel should be used to achieve self-compatibility [15, 16]. In order to attain self-compacting mortar, additional cementitious materials such as silica fume, chemical admixtures like superplasticizers, and reinforcing fibers need to be incorporated [17]. The density and homogeneity of the mortar, as well as the workability of the fresh mixture, can be enhanced by incorporating supplementary cementitious materials (SCMs) [18]. Although SCMs like silica fume enhance mortar properties, research is limited on the optimal use of these materials in varying proportions and their interaction with fibers.

Silica Fume (SF) is a secondary product generated from the manufacturing processes of silicon and ferrosilicon, known for its ultrafine spherical particles measuring between 0.1 to 0.2 μm in diameter. These particles are substantially smaller than typical cement particles. Owing to its high degree of fineness and substantial silica content, coupled with a large proportion of amorphous SiO_2 (85-90%), silica fume is recognized as an exceptionally reactive pozzolanic substance. This reactivity is further exhibited through pozzolanic reactions that transform calcium oxide $\text{Ca}(\text{OH})_2$ lime into additional calcium silicate hydrate, thus leading to a finer pore structure and less permeability [19]. In addition, the use of

silica fume in cementitious systems leads to a significant improvement in several properties of mortars [20-27]. Furthermore, there is a lack of comprehensive studies on how different silica fume contents affect the long-term durability and structural performance of fiber-reinforced Self-Consolidating Repair Mortars (SCRM). Additionally, the effectiveness of incorporating locally available materials in hot climate conditions has not been extensively explored.

Concrete reinforced with fibers such as polypropylene fiber (PPF) [28, 29], is widely acknowledged for its superior deformation characteristics, such as better abrasion resistance and ductility, minimal shrinkage, and enhanced flexural strength.

This paper examines various properties of mortar incorporating silica fume and polypropylene fibers. The properties of mortar include slump flow, V-funnel test, compressive and flexural strength, elastic modulus, water absorption, shrinkage, and bond strength. This study aims to develop a self-compacting concrete (SCC) mix specifically tailored for hot climate conditions using locally available materials.

Additionally, it seeks to classify the resulting self-consolidating repair mortars according to the EN 1504-3 standard [30] to ensure its suitability as a repair material. The research is intended to enhance the optimization of SCC for practical use in regions with challenging environmental conditions, thereby contributing to the advancement of durable and effective repair solutions in extreme climates

2. MATERIALS AND METHODS

Matrix constituents comprised several components, namely Ordinary Portland cement (OPC), silica fume (Fig. 1), fine aggregates, water, super-plasticizer, and polypropylene fiber. OPC, which adheres to the EN 197-1 standard [31], was utilized for mixture preparation. The material exhibited a Blaine fineness measure of 3850 cm^2/g and showed an average compressive strength of 42.5 MPa at 28 days. The Silica Fume (SF) used in this research adhered to the standards specified in EN 13263-1 [32] and EN 13263-2 [33] and had an average particle size between 0.1 to 0.3 μm . Table 1 shows the chemical compositions of both (OPC) and (SF).

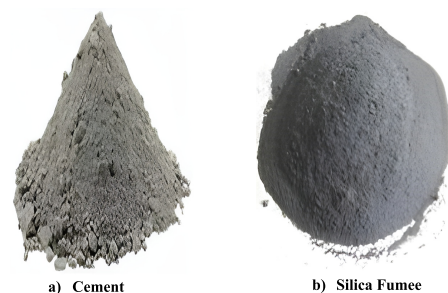



Fig. (1a, b). Raw materials used.

Table 1. Chemical and physical properties of OPC and silica fume.

Chemical Composition %	OPC	Silica Fume
CaO	61.74	< 0,1
SiO ₂	20.92	≥ 85
Fe ₂ O ₃	3.43	≤ 1%
Al ₂ O ₃	5.60	≤ 1%
MgO	1.7±0.5	≤ 1%
SO ₃	2.5±0	≤ 2,0
Cl-	0.02-0.05	≤ 0,1
Na ₂ O	0.1	≤ 1,0
Loss on ignition	8±2	≤ 4,0

Table 2. Characteristics of PP fibers.

Photo	Length (mm)	Diameter (µm)	ElasticModulus (GPa)	Elongation (%)	Tensile strength (GPa)	Density (g/cm ³)
	12	30	3	50	0.5	0.9

For creating Self-Consolidating Repair Mortars (SCRMs) mixtures in this study, natural river sand was utilized, characterized by a fineness modulus of 2.82 and a bulk specific gravity of 2.70. The mixing water came from local tap water sources, and to enhance the mixtures' dispersion, a high-range water-reducing superplasticizer (MEDAFLOW 30) with a density of 1.07 kg/m³ was incorporated. Additionally, polypropylene fiber (PPF) measuring 12 mm in length was employed. The principal

attributes of the PPF are comprehensively listed in Table 2.

In this study, a total of five different mortar mixtures were formulated. Specific mix proportions for both the repair mortars and the substrate mortar (SUBM) are shown in Table 3. Additionally, to modify the properties of these mixtures, different percentages of silica fume (SF) were incorporated based on the weight of the cement, ranging from 0% to 20%.

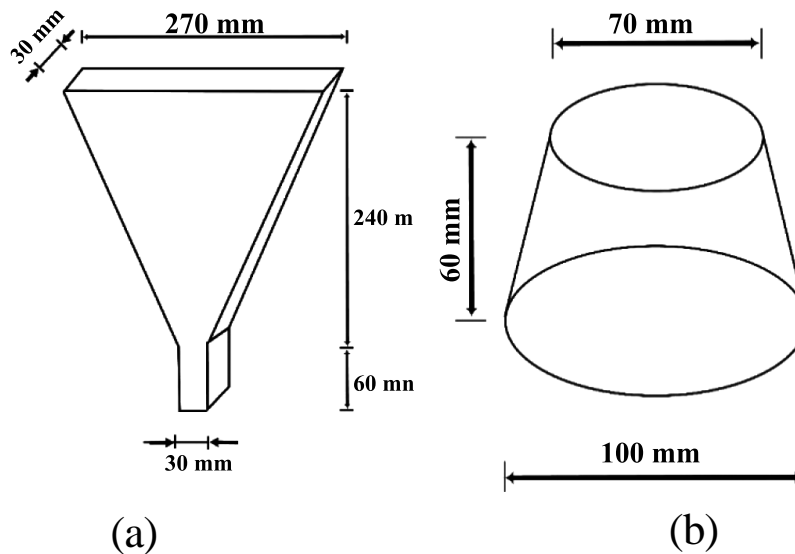


Fig. (2). Deformability test for fresh mortar: (a) V-funnel flow test (b) The mini-slump flow test.

Table 3. Mix proportions for mortar with varying replacement levels per 1 m³.

Name of the Repair Mortars	Cement (OPC) (kg)	Silica Fume (kg)	Water (kg)	Sand (kg)	Water-to-powder Ratio (W/P)	Super Plasticizer (%)	PPF Fiber (%)
SCRM0	767	000	317	1166	0,45	0,7	0,2
SCRM5	728	038	319	1166	0,45	0,9	0,2
SCRM10	690	077	314	1166	0,45	1,2	0,2
SCRM15	652	115	313	1166	0,45	1,5	0,2
SCRM20	613	153	309	1166	0,45	2,4	0,2
SUBM	525	000	340	2250	0,64	1,2	0,0

The methodology for preparing these mortar mixtures involved the following steps: First, (SF) and sand were blended for a period of 30 seconds. Then, 70% of the predetermined water quantity was incorporated and mixed for one minute. After that, the remaining water, which contained the superplasticizer, was added, and the mixture was stirred for an additional minute. In the third step, in accordance with the technical guidelines provided by the manufacturer, the Polypropylene Fibers (PPF) were manually dispersed into the mixture and mixed for a duration of 5 minutes. Finally, after a curing period of 24 hours from the casting process, all molds were removed and then transferred to a curing room. It is worth noting that all specimens, except for the shrinkage specimens, were continuously immersed in water throughout the testing period.

3. EXPERIMENTAL

3.1. Deformability Test for Fresh Mortar

In this experimental investigation, we evaluated the workability of Self-Consolidating Repair Mortar (SCRM) using two specific tests: the v-funnel flow test (depicted in Fig. 2a) and the mini slump flow test (Fig. 2b). The tests were performed following the guidelines set by EFNARC [34].

The mini-slump flow test apparatus featured specific dimensions, including a bottom diameter of 100 mm, a top diameter of 70 mm, and a height of 60 mm. For the test, fresh mortar was filled into this cone, which was positioned at the center of a marked glass plate. When the cone was lifted vertically, the spread diameter of the mortar was measured and calculated as the average of two perpendicular dimensions.

In the V-funnel flow test, the procedure began by pouring the mortar completely into the funnel. Once filled, the bottom outlet was opened to let the mortar flow out. The time taken from the start of the flow to when the mortar began to exit from the bottom outlet was recorded and denoted as "t," representing the V-funnel flow time. It is worth noting that in accordance with EFNARC acceptance criteria, the workability values for SCMs were expected to fall within the range of 240-260 mm for slump-flow diameter and 7-11 seconds for V-funnel flow time.

3.2. Compressive and Flexural Strengths

Moreover, to evaluate the flexural and compressive strengths, prism specimens of dimensions 40×40×160

mm³ were prepared for each mortar mixture, adhering to the procedures specified in EN 12190-5 [35]. These assessments were performed at four different time intervals: 2, 7, 28, and 90 days. For accuracy, the flexural strength results were derived by averaging values obtained from three flexural samples, and the compressive strength results were calculated from six compression samples (Fig. 3).



Fig. (3). Flexural and compressive strength test.

3.3. Elastic Modulus

In addition to strength evaluations, the elastic modulus was also determined in accordance with the EN-12504-4 [36]. This involved the preparation of cylindrical specimens, each having dimensions of 40 mm in diameter and 80 mm in length, were created. Following a period of 24 hours from the initial casting, all the molds have been unmolded. The specimens were then immersed in water until they reached their designated testing ages, which were 2, 7, 28, and 90 days. After this period, to precisely measure their density, the specimens were subjected to a 24-hour oven-drying process at a temperature of 105°C. The propagation velocity of ultrasonic waves through these specimens, which is influenced by their density, was determined using an ultrasonic testing method.

The disposition of the transducers within the specimen using the direct transmission method is illustrated in Fig. (4). Additionally, to ensure precise ultrasonic results, a flat surface was achieved by employing a smooth diamond saw to create a bonded plane.



Fig. (4). The process of measuring the propagation velocity of ultrasonic waves through the specimen.

The dynamic elastic modulus (ED) can be calculated using Eq. (1) as follows:

$$ED = \rho V^2 \tag{1}$$

Here:

- E_D represents the elastic modulus in GPa.
- ρ denotes the density of the dry specimens in kg/m^3 .

- V stands for the sound speed in km/s.

3.4. Absorption

The absorption test was used in this investigation in accordance with EN 1015-18 [37]. Half-prism specimens measuring $40 \times 40 \times 80$ mm³ were prepared to assess the capillary absorption coefficient after 28 days. Following a 28-day curing period, the specimens were subjected to a 24-hour oven-drying process at a temperature of 105°C to ascertain their dry mass (W). Afterward, all surfaces of the specimens, excluding their top and bottom sides, were coated with epoxy resin. This sealing was done in a manner that allowed water penetration in only one direction, as visually demonstrated in Fig. (5).

3.5. Shrinkage

Furthermore, to assess drying shrinkage, we utilized three prism specimens, each containing embedded copper heads at their two longer ends in accordance with EN 12617-4 [38]. Initially, these specimens were placed in molds and wrapped with plastic paper for one day during the curing process. Following this initial curing period, the samples were carefully extracted and sealed with adhesive bands at both ends to minimize water evaporation. Subsequently, these specimens were stored in our laboratory under controlled conditions, maintaining a temperature of 23°C and a relative humidity (RH) of 55%.

For precise shrinkage measurements, we employed a shrinkage measurement frame equipped with a micrometer precision comparator. It is worth noting that autogenous shrinkage, caused by the cement hydration process, results in reduced relative humidity within the pores of the specimens. When curing is conducted in an open environment, the movement of water through these pores to the surface, combined with water loss from the surface due to evaporation, leads to additional shrinkage.

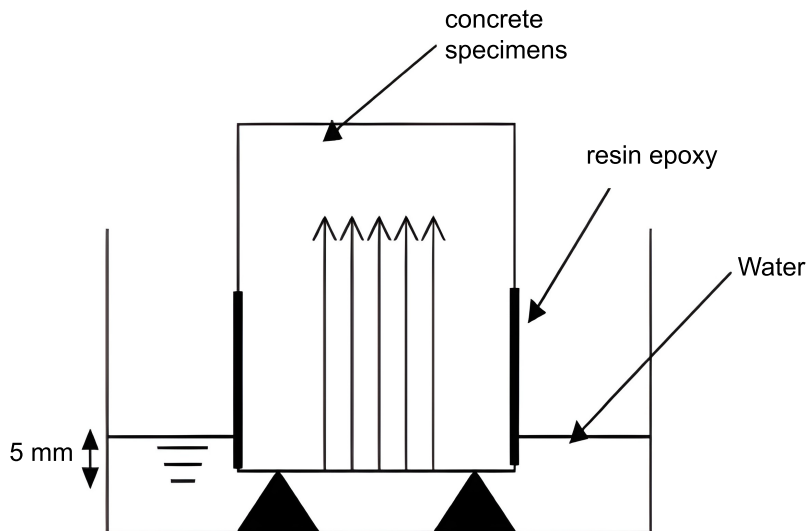


Fig. (5). Schematic diagram of water absorption test.

Positioning of the specimen within the measuring frame is visually depicted in Fig. (6). Shrinkage strain measurements were carried out for all mixtures up to a duration of 90 days.



Fig. (6). Frame to measure shrinkage deformation.

3.6. Flexural Bond Strength

The bond strength between the repair materials (Self-Compacting Repair Mortars, SCRM) and the substrate mortar (SUBM) was assessed using a three-point bending test. This test was conducted in accordance with the ASTM C78 [39] guidelines. In this test, composite specimens, consisting of SCRM and SUBM, were

prepared. Each specimen was composed of two prism halves, each measuring $40 \times 40 \times 80 \text{ mm}^3$. One half was constructed using SCRM and was securely bonded to the other half using SUBM, as visually depicted in Fig. (7a).

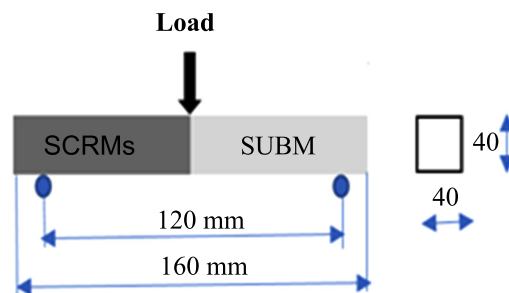
The substrate portion of the specimen was cast within metallic molds and subjected to a 28-day curing process in water, maintained at a controlled temperature of $20 \pm 2 \text{ }^\circ\text{C}$. In addition, to ensure a robust adhesion of the repair material, the surface of the substrate mortar ($40 \times 40 \text{ mm}^2$) was carefully prepared by brushing.

Before casting the SCRM, the interfaces between the substrate and repair materials were immersed in water for a period exceeding 6 hours. Upon reaching 28 days of age, the repair mortars were cast onto the peak of the substrate. During the testing procedure, each composite specimen was positioned centrally between two plates of the testing apparatus, and a load was applied at a constant rate of 0.5 kN/s until the point of failure, as illustrated in Fig. (7b).

Additionally, the compatibility between the SCRM and the SUBM was evaluated based on the failure mode exhibited by the composite samples. If the fracture occurred along the interface between the repair material and the substrate, it was classified as an incompatible failure (adhesive failure). Conversely, if the failure occurred within the repair material (cohesive failure), it indicated that the repair material was compatible with the substrate mortar. The bonding strength between the existing and new materials plays a pivotal role in determining the quality of the repair material.



(a)



(b)

Fig. (7). (a) Preparation of composite sample, (b) Third- point's loading composite prism.

Table 4. Fresh property of SCRMs.

Repair Mortar	Mini Slump (mm)	EFNARC Specifications	Mini V-funnel (sec)	EFNARC Specifications	Dosage of superplasticizer (%)
SCRM 0	245	Between 240 to 280 mm	5,33	Less than 11s	0,7
SCRM 5	240		5,32		0,9
SCRM 10	270		4,26		1,20
SCRM 15	255		5,23		1,50
SCRM 20	277		4,43		2,40

4. RESULTS AND DISCUSSION

4.1. Deformability Test for Fresh Mortar

Table 4 presents the Mini-slump and mini-funnel values corresponding to the various SCRMs mixtures.

The optimum dosage, commonly known as the saturation dosage of superplasticizer, is the dosage at which there is no further increase or alteration in the spread of the slump flow of the mixtures. Fig. (8) provides a visual representation of the varying superplasticizer dosage levels.

It should be noted that the addition of SF to the mortar results in lower performance compared to the control mixture SCRM0 in terms of fresh characteristics. The greater surface area and reduced particle size of Silica

Fume (SF) resulted in an increased demand for water in the mortar mix, resulting in reduced workability of the fresh mortar. Additionally, to maintain a consistent slump flow for all repair mortars (SCRMs), it was necessary to increase the dosage of superplasticizer. Table 4 displays the slump flow diameters for all mixtures, falling within the range of 240 to 270 mm. According to EFNARC guidelines, a diameter between 240 and 260 mm is considered acceptable [34]. Yaseri *et al.* [40] recommended a mini-slump range of 220-280 mm, and for this study, the acceptable mini-slump flow was determined to be within the range of 240-270 mm. Consequently, a superplasticizer had to be added to enhance workability. Increasing the superplasticizer dosage resulted in an 80% convergence of the mini-slump flow toward the specified threshold.

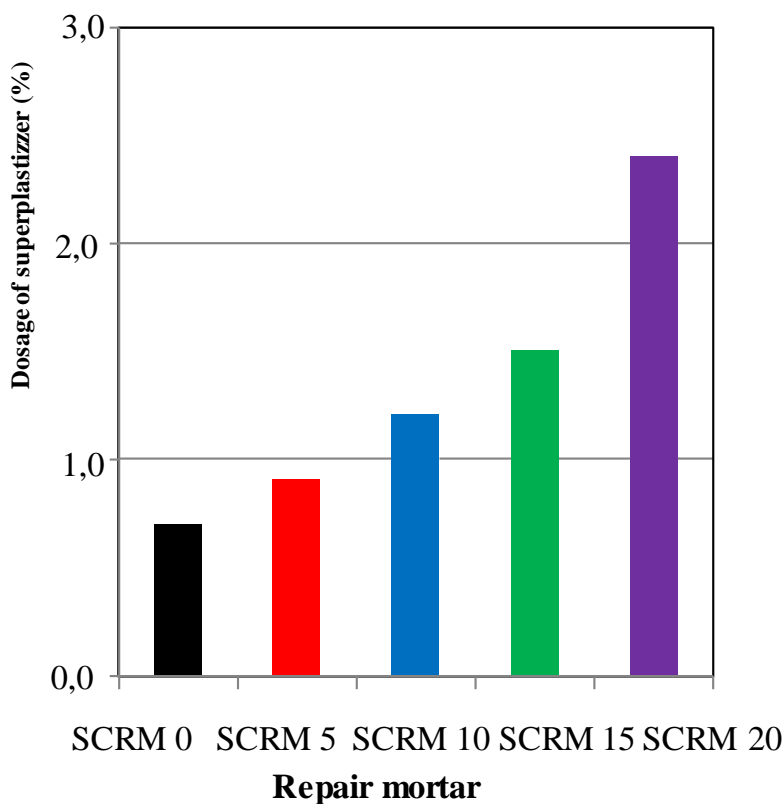


Fig. (8). Variation of dosage of superplasticizer (%).

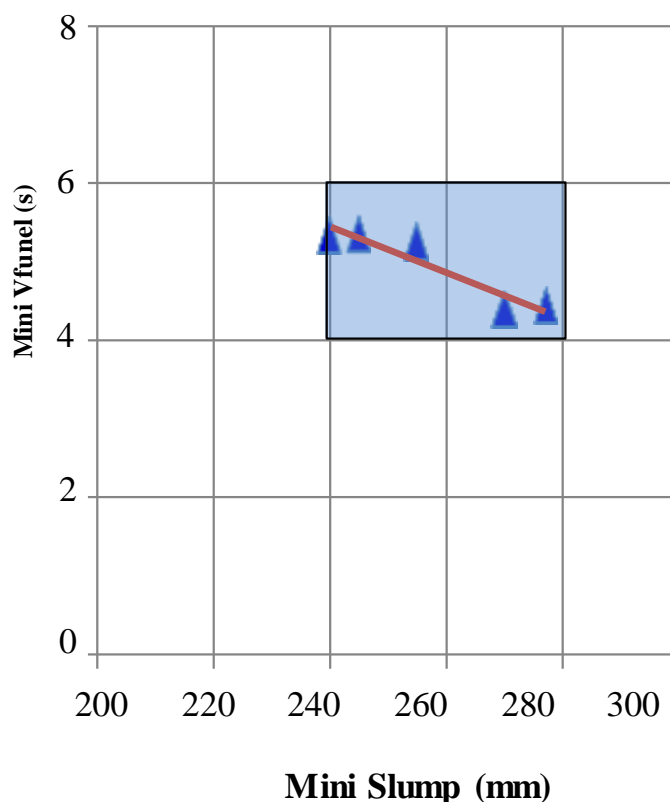


Fig. (9). Correlation between mini-slump flow and mini V-funnel tests for SCRMs.

As indicated in Table 4, the flow time values for all SCRMs mixtures ranged from 4.26s to 5.32s. The incorporation of SF content resulted in diminished workability of the fresh repair mortar, thereby requiring the addition of a superplasticizer to enhance its workability. The results revealed that Fiber-Reinforced Mortars (FS) decreased the fluidity of SCRM mixtures, with the most significant impact observed at a dosage of 20%. This finding aligns with the conclusions drawn by Erdogdu *et al.* [41]. Additionally, the presence of SF increased the superplasticizer requirement in mortars [42]. The expansive surface area of SF particles led to heightened adsorption of the superplasticizer. This phenomenon reduced the superplasticizer's presence in the solution surrounding cement particles, subsequently impacting the fluidity of the cementitious mixtures [43]. This aligns with the results documented in previous studies [44, 45]. Furthermore, a pronounced linear relationship was observed between the mini V-funnel spread and the mini-slump spread, as depicted in Fig. (9). Notably, when the mini-slump spread ranged from 240-280 mm, the corresponding mini V-funnel time was observed to be between 4 to 6 seconds.

In theory, the workability of fresh cementitious pastes can be characterized by the values derived from both the slump flow and mini V-funnel test results. As a result, it can be noted or concluded that the filling results can be

used to predict the workability of SCRM and that there is a connection between the filling capacity and the workability of SCRM.

4.2. Compressive and Flexural Strengths

Data on the flexural and compressive strengths are presented in Table 5. Figs. (10 and 11) showcase the flexural and compressive strengths of Self-Consolidating Repair Mortar (SCRM) mixtures, incorporating varying Ferrosilicon (FS) content levels of 5%, 10%, 15%, and 20%, measured at 2, 7, 28, and 90 days.

Fig. (10) displays the flexural strength of repair mortars (SCRMs) mixtures with different FS contents of 5%, 10%, 15%, and 20% at testing intervals of 2, 7, 28, and 90 days.

Conversely, at the 90-day interval, SCRM5 demonstrated the highest compressive strength, followed by SCRM10, and then SCRM0. The compressive strengths of SCRM5 and SCRM10 were closely matched (73.9 MPa for SCRM5 and 72.4 MPa for SCRM10). This trend is primarily attributed to the pozzolanic reaction, which contributes to a denser microstructure within the mix, thus enhancing the compressive strength over a longer period.

This demonstrates that the SF dosage increased pozzolanic activity, resulting in enhanced hydration and compressive strength at late ages.

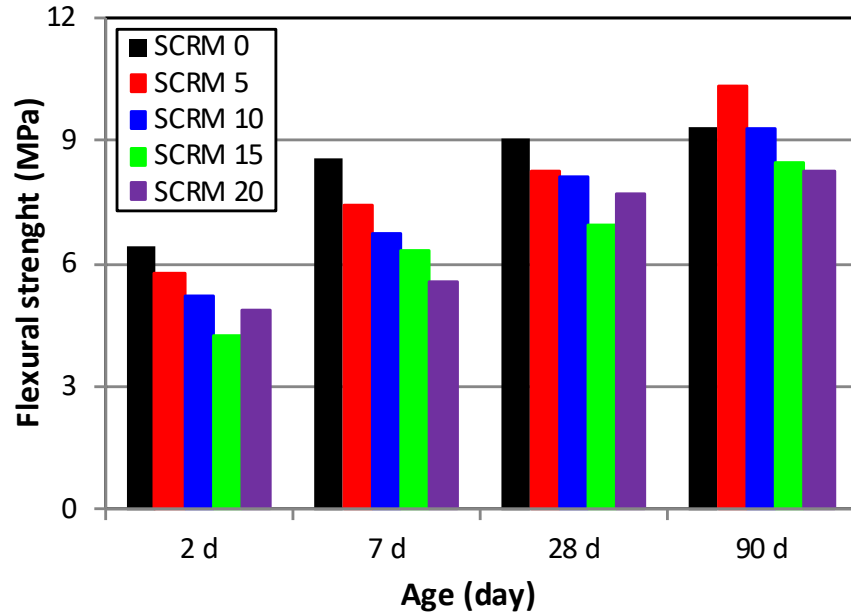


Fig. (10). Influence of SF content on flexural strengths of repair mortars (SCRMs) over various curing periods.

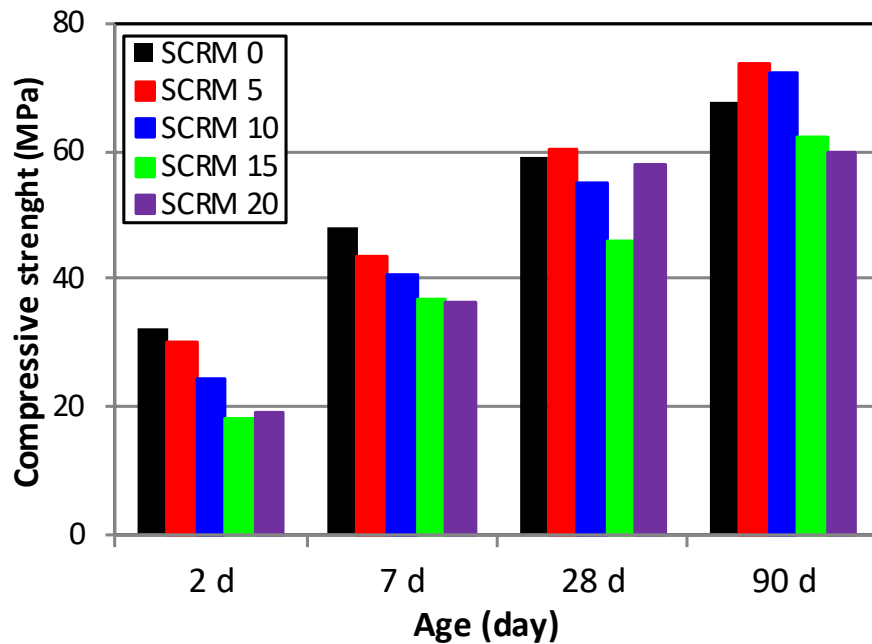


Fig. (11). Illustrates the impact of SF content on the compressive strengths of SCRMs.

At 28 days, all SCRMs displayed compressive strengths comparable to that of SCRM0, except for the SCRM15 mixture.

The information depicted in Fig. (10) indicates an increase in the flexural strength of Self-Consolidating Repair Mortars (SCRMs) over time. However, there was a

notable decrease in flexural strength with higher Silica Fume (SF) content. Specifically, the control mixture (SCRM0) demonstrated greater flexural strength at 28 days compared to other SCRM mixtures. Furthermore, between 28 to 90 days of curing, SCRM5 and SCRM10 showed an increase in flexural strength by 25.5% and 14.4%, respectively.

Table 5. Hardened properties of SCRMs.

Repair Mortar	Flexural Strength (MPa)				Compressive Strength (MPa)				Elastic modulus (GPa)			
	2 d	7 d	28 d	90 d	2 d	7 d	28 d	90 d	2 d	7 d	28 d	90 d
SCRM 0	6,44	8,59	9,06	9,36	32, 3	48,0	59,1	67,8	21,30	25,40	27,30	33,76
SCRM 5	5,77	7,41	8,26	10,37	29, 9	43,6	60,4	73,9	19,03	24,27	27,43	32,73
SCRM 10	5,23	6,71	8,11	9,28	24,3	40,5	55,1	72,4	16,33	23,79	26,31	29,22
SCRM 15	4,21	6,32	6,94	8,50	18,1	36,6	46,1	62,1	14,76	21,21	24,39	29,87
SCRM 20	4,84	5,54	7,72	8,27	19,0	36,4	57,9	59,8	15,83	24,94	28,07	28,01

It should be noted that the ideal proportion of superplasticizer to SF for achieving self-compacting mixes is typically around 1% of the binder weight and 10% of the weight of the binder, respectively. This combination serves to reduce porosity while enhancing strength. Furthermore, the incorporation of SF and superplasticizer enhances the pozzolanic reaction at 28 days. Additionally, the development of a denser microstructure in the mortar, with reduced porosity, can lead to increased strength and enhanced durability.

Early strength development in cementitious systems is generally less affected by SF. SF, being a pozzolanic substance, primarily contributes to long-term strength characteristics while potentially reducing flexural strength at an early age. Importantly, in the initial stages of strength development, fiber-reinforced concrete typically exhibits lower compressive and flexural strengths relative to standard concrete.

As for Fig. (11), it shows that the development of compressive strengths follows a similar pattern to that of flexural strengths. At early ages (2 days of curing), (SF) was found to adversely affect the compressive strength of SCRMs, with all SCRMs showing reduced compressive strength compared to SCRM0. For instance, at the 7-day mark, there were observed decreases in compressive strength by 9.2%, 15.6%, 23.8%, and 24.2% for SCRMs5, SCRM10, SCRM15, and SCRM20, respectively, relative to SCRM0. This reduction is largely due to the dilution effect caused by SF.

Numerous studies have noted that the impact of silica fume (SF) on strength development in mortar is more pronounced after the first 7 days [45-48]. Initially, an increase in SF content up to a certain threshold tends to enhance the compressive strength of the mortar. However, exceeding this threshold leads to a decline in strength as the SF content increases further [49]. It has been discovered in other research that the addition of silica fume to water does not directly participate in the hydration reactions of cement. Rather, it interacts with the $\text{Ca}(\text{OH})_2$ produced during the hydration process, forming hydrated calcium silicates (C-S-H gel). This process effectively improves the microstructure of the cementitious matrix once it has hardened, resulting in a more compact and dense structure, which is beneficial for early strength development and contributes to the improved strength and durability of the mortar over time [50].

Optimal concrete strength at 28 days is achieved with a superplasticizer (SP) concentration between 1.0-1.2% and an SF content of 10-15% by binder weight. Furthermore, the use of 15% SF as a replacement enhances the concrete's durability and strength, as demonstrated in Fig. (9). This enhancement is likely due to SF's high pozzolanic activity, stemming from its significant amorphous SiO_2 content.

These findings align with those reported by other researchers [51, 52].

However, compressive and flexural strength development increases even more after 28 days for SCRMs mixes with 5-10% SF replacement and continues at a later time due to the pozzolanic reaction.

The correlation between compressive and flexural strengths, as outlined by various researchers, can be summarized in a different way Eq. (2).

$$f_t = k f_c^\alpha \quad (2)$$

Where f_c represents compressive strength in MPa and f_t is flexural strength in MPa. The correlation between compressive and flexural strength findings proposed in this study, represented by Eq. (3), was used to model the correlation among compressive and flexural strength for SCRMs mixtures.

Coefficients k and α were obtained through nonlinear regression analysis using the test results, which were considered as the main variables. The values obtained were k and α by nonlinear regression analysis are 0.872 and 0.55, respectively. The corresponding strong correlation coefficient $R^2 = 0,930$ can be expressed as follows:

$$f_t = 0,872 \cdot f_c^{0,55} \quad (3)$$

Eq. (3), shown in Fig. (12), can be used to estimate and predict the bending strength from the corresponding compressive strength value, with high reliability.

4.3. Elastic Modulus

Elasticity modulus for repair mortar was assessed at intervals of 2, 7, 28, and 90 days, utilizing cylindrical specimens, as demonstrated in Fig. (13).

The dynamic elastic modulus of SCRMs mixtures, which characterizes the material's stiffness, is an essential material characteristic and plays a pivotal role in engineering design and the development of materials.

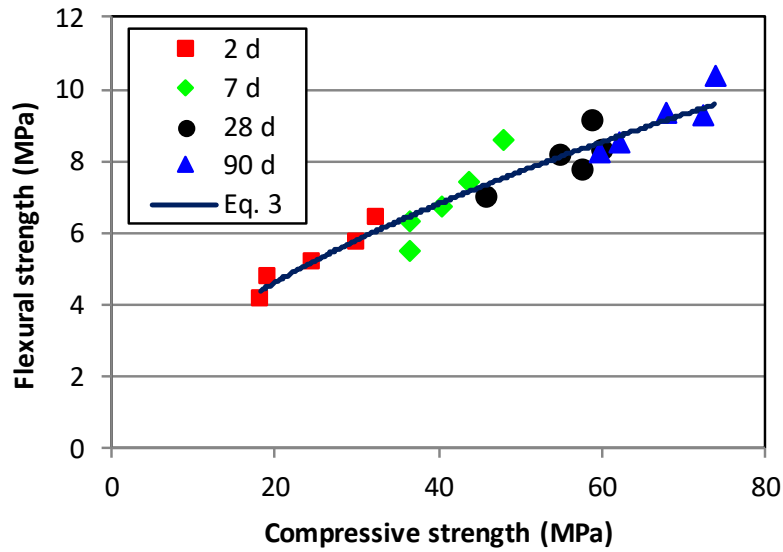


Fig. (12). Relation among flexural strength and compressive strengths of SCRMs.

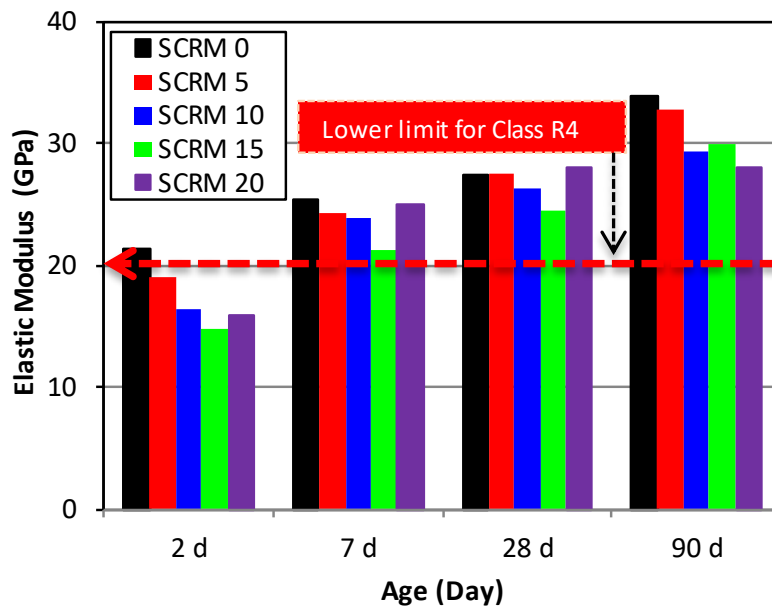


Fig. (13). Influence of SF content on elastic modulus of SCRMs.

Measurements showed that the elastic modulus varied from 28.01 to 33.76 GPa at 90 days. Clearly, employing high-volume Silica Fume (SF) led to a decrease in the dynamic modulus of elasticity compared to SCRM0, which showed the highest modulus. On the other hand, the elastic modulus of all Self-Consolidating Repair Mortar (SCRM) mixtures exhibited an increase over time, particularly noticeable after 90 days of curing. For example, during the extension of the curing period from 28 to 90 days, the elastic modulus of SCRM0 and SCRM15 increased by 24% and 22%, respectively. These findings

generally align with those reported in prior studies [53, 54]

Various models and correlations have been suggested in the literature to estimate the modulus of elasticity of concrete, predominantly based on the concrete's compressive strength.

This study has formulated an empirical correlation between the modulus of elasticity and compressive strength, which can be expressed as follows:

$$E_c = 3,162 f_c^{0,537} \tag{4}$$

Here, f_c is the compressive strength in MPa and E_c is the elastic modulus in GPa.

Eq. (4) demonstrates a strong correlation between elastic modulus and compressive strength, as evidenced by a coefficient of determination (R^2) exceeding 0.92. Fig. (14) further shows a remarkable correlation between the compressive strength and the modulus of elasticity.

4.4. Water Absorption

Fig. (15) presents the capillary absorption coefficients

for different Silica Fume (SF) concentrations at 28 days, examining sorptivity, which evaluates a porous material's capacity for water absorption and transmission through capillary action, to gauge the durability characteristics.

The graph in Fig. (15) indicates a reduction in the capillary absorption coefficient with an increase in SF content up to 10%. For instance, the coefficient for SCRM5 was 60% lower than that of SCRM0. Conversely, this coefficient substantially rose when SF levels exceeded 10%, reaching 20%.

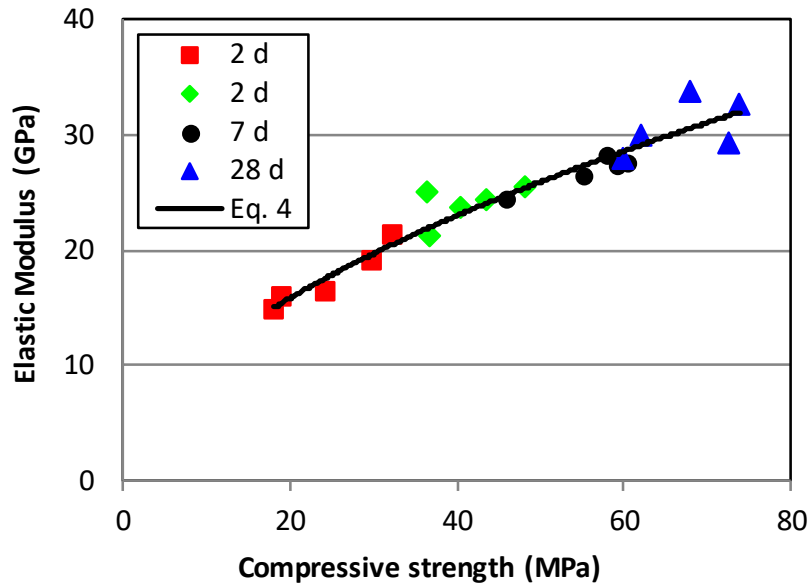


Fig. (14). Relationship between the elastic modulus and compressive strengths of SCRMs, described by Eq. (4).

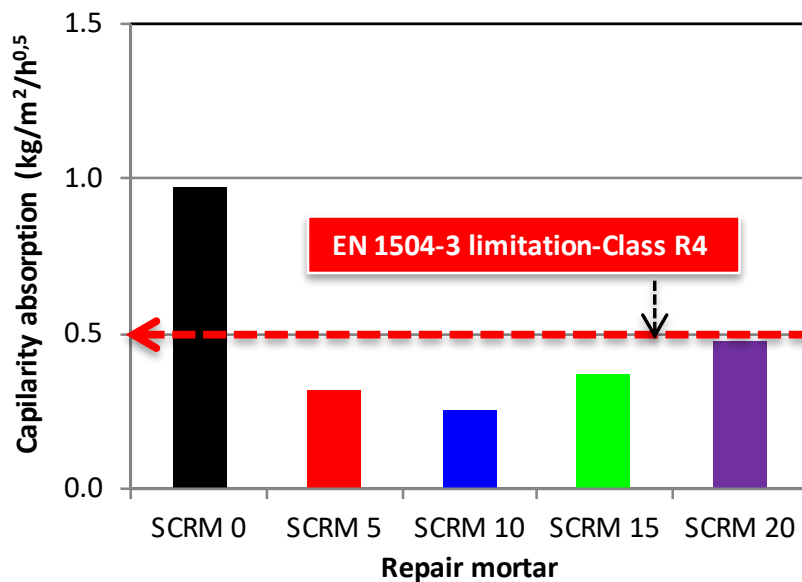


Fig. (15). Influence of SF content on the capillary absorption coefficient of SCRMs after 24 hours.

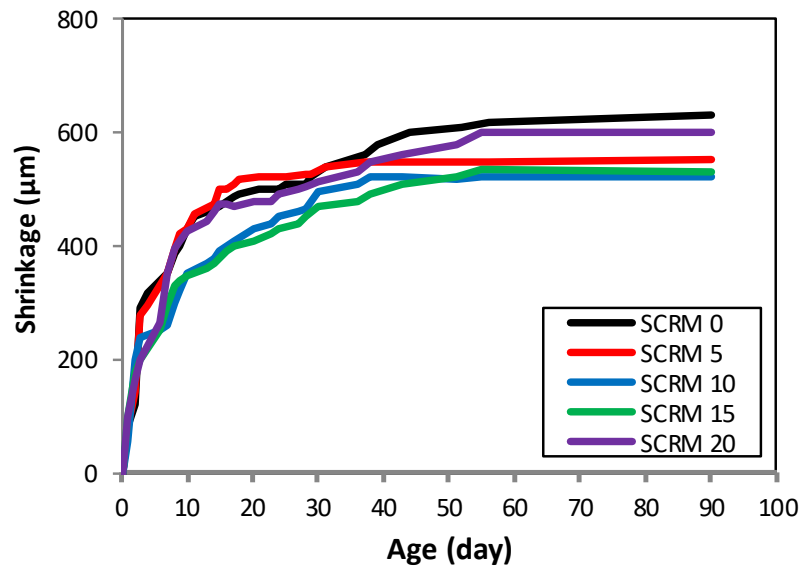


Fig. (16). Displays the impact of SF content on drying shrinkage of SCRMs.

These findings suggest that SF integration diminishes surface pores and imperfections in the mortar relative to the standard repair mortar (SCR M0), implying that a rise in SF content up to 20% diminishes SCRMs mortar's porosity. At 10% SF concentration, the capillary absorption coefficient dropped to $0.27 \text{ (kg/m}^2 \cdot \text{h}^{0.5})$, marking a 71% decrease from SCR M0. Thus, SF addition effectively lowers water absorption in the repair mortar.

Indeed, the capillary absorption coefficient for all repair mortars SCR Ms that range between 0.27 and $0.46 \text{ kg/m}^2 \cdot \text{h}^{0.5}$ satisfy the requirements (less than $0.5 \text{ kg/m}^2 \cdot \text{h}^{0.5}$) for building materials designed for use in Class R4 structural applications. The following reasons can explain these results. Firstly, the potent pozzolanic activity of Silica Fume (SF) is instrumental in compacting the microstructure of Self-Consolidating Repair Mortars (SCR Ms), thereby lessening their porosity *via* the generation of calcium-silicate-hydrates (C-S-H). Secondly, the comparatively larger specific surface area of SF, in relation to cement, contributes to a decrease in water absorption by further compacting the mortar matrix.

Practically, this suggests that the addition of SF particles primarily serves to occupy the spaces among the hydrated cement particles, leading to enhanced compressive strength and a reduction in water absorption. Notably, the control mix SCR M0 demonstrated the highest capillary absorption coefficient. In contrast, all SF-inclusive SCR Ms showed markedly lower capillary absorption coefficients compared to SCR M0. These observations are in line with findings from various other studies [43, 55, 56].

4.5. Drying Shrinkage

Fig. (16) displays the drying shrinkage data for all Self-Consolidating Repair Mortar (SCR M) mixtures over a period of 90 days. The figure reveals that increasing Silica Fume (SF) content to 10% leads to a reduction in the drying shrinkage of SCR Ms at 90 days. For instance, SCR M10

showed a 33% decrease in 90-day drying shrinkage compared to SCR M0. However, it is important to recognize that using more than 10% SF in the mix might cause the specimens to expand.

Previous studies have consistently found that SF usage tends to diminish the drying shrinkage of repair mortars. This effect can be attributed to several factors. Firstly, the addition of pozzolanic materials lowers the amount of cement needed, which in turn reduces the heat of hydration and, consequently, the shrinkage of the mortar mixes [57, 58].

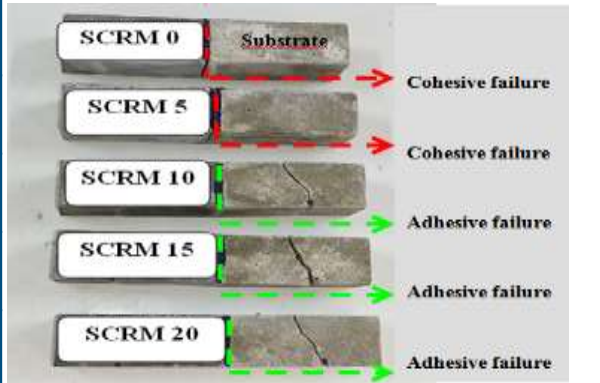
Secondly, after sufficient curing, the shrinkage of SCR Ms containing SF generally decreases due to the pozzolanic reaction, which generates extra C-S-H gels, thereby making the matrix denser and slowing the rate of water loss. Thirdly, the use of SF contributes to shrinking reduction by reducing the diameter and connectivity of pores, a process partly influenced by SF's reinforcing properties.

In summary, these findings suggest that mortars containing pozzolanic materials exhibit lower drying shrinkage than control mixes under air-cured conditions.

4.6. Flexural Bond Strength

Table 6 provides insights into how SF influences the adhesion of composite samples (SCR M/SUBM) under normal water curing conditions. Raising SF content positively influences the bonding interaction between mortar substrates and the repair mortar. Compared to the control mix, substituting cement with 10%, 15%, and 20% Ferrosilicon (FS) resulted in a notable enhancement in the flexural bond strength of (SCR M) specimens. Specifically, this substitution led to improvements in bond strength by 149%, 133%, and 111% for 10%, 15%, and 20% FS replacements, respectively. The highest value, 8.14 MPa, was achieved by SCR M10. Additionally, the results of the 28-day bonding process indicated that composite samples can generally be categorized into two failure types.

Table 6. The bond flexural strength of SCRMs.

Repair Mortars (SCRMs)	Bond Flexural Strength (MPa)	Failure Mode
SCRM 0	3,27	
SCRM 5	6,01	
SCRM10	8,14	
SCRM 15	7,63	
SCRM 20	6,90	

In specific terms, the failures occurred in the substrate of the composites SCRM10/SUBM, SCRM15/SUBM, and SCRM20/SUBM, which indicates a strong bond between SCRM mortar and SUBM. In contrast, at 0% and 5% FS content, the interface cracked, and the repair mortar completely separated from the support (resulting in cohesive failure). The interfacial transition zone, which is the boundary between the old mortar and the new repair materials, can be enhanced by the inclusion of Polypropylene Fiber (PPF) [59]. It is also important to mention that in the restoration of concrete structures, the tensile bond strength of the repair materials should ideally surpass 2.1 MPa [60].

On the other hand, A-lite (C_3S), B-lite (C_2S), and ferrite (C_4AF) are the three primary components of cement, and their hydration accelerates these positive effects. Following the cement hydration process, the free alkali, primarily in the form of calcium hydroxide ($Ca(OH)_2$), reacts with the silica component in Silica Fume (SF), a process that is facilitated by the presence of water. This reaction results in the formation of calcium silicate hydrate (C-S-H), contributing to a decrease in capillary porosity while simultaneously reducing the calcium hydroxide content within the matrix [61]. Silica Fume's larger surface area, which enhances its reactivity, effectively fills voids in both interfacial and interfacial transition zones, leading to a denser and more uniform structure. Furthermore, the robust bond between Self-Consolidating Repair Mortars (SCRMs) and substrate mortars (SUBMs) helps to prevent crack propagation in the transition zone [62].

It is important to recognize that variables such as the nature of the bonding agent, the cleanliness and moisture level of the substrate surface, and the roughness of the interface can significantly affect adhesion at the interface [63]. In line with these findings, adding Silica Fume (SF) to the mortar not only improves the mechanical characteristics of the interfacial transition zones but also strengthens the bond between the repair mortar and the substrate, leading to a more robust bond [62].

The addition of SF enhances the internal pore structure

and compactness of the mortar, which in turn significantly boosts its durability. This increased durability plays a crucial role in reducing mortar degradation in harsh environments, thereby extending their service life [64].

CONCLUSION

The findings of the experimental study investigating the effects of SF and PPF fiber on self-compacting repair mortar behavior lead to the following conclusions:

- The inclusion of silica fumes notably influences the workability of self-consolidating repair mortars (SCRMs), with workability decreasing as the SF content
- Hardened properties of SCRMs are decreased when high-volume silica fume is used, regardless of age. Moreover, due to the pozzolanic reaction, after 90 days, all SCRM mixtures demonstrate significantly higher flexural and compressive strengths.
- At 90 days, SCRM5 and SCRM10 have compressive strength values of 73.9 and 72.9 MPa, accordingly, which can satisfy class R4 requirements according to EN 1504-3 [30]. In addition, all the SCRM mixes produced in this study showed strengths in excess of 40 MPa at 90 days, making them suitable for a large number of different applications.
- A predictive model has developed successfully for the relationship between compressive and flexural strengths of SCRMs, with a high correlation coefficient $R^2=0.930$. This model provides a reliable method for estimating flexural strength from compressive strength, offering valuable insights for practical applications of SCRMs.
- Lower elastic modulus readings observed in the SCRM mixtures are advantageous for mortar restoration and help mitigate the internal stresses induced by shrinkage, which is beneficial for the restoration process.
- The study presents a refined empirical model for correlating the modulus of elasticity with compressive strength. The high determination coefficient ($R^2>0.92$) confirms the model's strong predictive capability, providing a valuable tool for estimating elastic modulus from compressive strength in concrete applications.
- Incorporating Silica Fume (SF) significantly influences

the capillary absorption coefficients of repair mortars. Up to a 10% SF concentration reduces capillary absorption by up to 71%, enhancing durability by decreasing porosity. However, SF levels exceeding 10% increase the absorption coefficient. Mortars with SF concentrations between 0.27 and 0.46 kg/m²·h^{0.5} meet the Class R4 standards for building materials, thanks to SF's pozzolanic activity and high specific surface area, which improve the material's microstructure and reduce water absorption.

- Increasing Silica Fume (SF) content up to 10% effectively reduces drying shrinkage in Self-Consolidating Repair Mortars (SCRMs), with a notable 33% decrease observed at 90 days for SCRMI0 compared to SCRMO. This reduction is attributed to SF's pozzolanic activity, which decreases the amount of cement needed, mitigates the heat of hydration, and promotes the formation of additional C-S-H gels, enhancing the density of the mortar matrix and reducing pore connectivity. However, higher SF contents beyond 10% may lead to increased expansion. Overall, incorporating SF results in lower drying shrinkage compared to control mixes, demonstrating its effectiveness in improving the dimensional stability of repair mortars.
- According to the three-point bending test, the SCRMI0 mixture using 10% silica fume showed a satisfactory binding strength with substrate, as the cure time increased. This enhancement in bonding power is a result of the pozzolanic reaction. The results imply that SCM is potentially a useful material for repairing damaged concrete structures. Failure continued to occur along the interface when 10% natural pozzolana was incorporated into the cement mix.
- According to the findings of this work, SCRMI0 is possibly a good repair material that complies with EN 1504-3 [30] due to its adequate mechanical capabilities and durability characteristics with the concrete substrate.
- Future research should explore the long-term durability of the SCRMs under diverse environmental conditions and compare the performance of silica fume with other supplementary cementing materials. Additionally, field studies and assessments of economic and environmental impacts will be valuable for validating and enhancing the practical application of these materials.

AUTHOR'S CONTRIBUTION

M.E.: Methodology, Experimental study, Investigation, Writing-original draft; M.G.: Writing - review & editing, Supervision, Conceptualization; S.C. and J.K.: Data Analysis and Interpretation.

All authors reviewed the results and approved the final version of the manuscript

LIST OF ABBREVIATIONS

SF	=	Silica Fume
SCRMs	=	Self-Consolidating Repair Mortars
SUBMs	=	Substrate mortars

CONSENT FOR PUBLICATION

Not applicable.

AVAILABILITY OF DATA AND MATERIALS

The data and supportive information are available within the article.

FUNDING

None.

CONFLICT OF INTEREST

Dr. Mohamed Ghrici is the Editorial Advisory Board member of The Open Civil Engineering Journal.

ACKNOWLEDGEMENTS

This research was sponsored by the General Directorate for Scientific Research and Technological Development (DGRSDT) of the Algerian Minister of Higher Education and Scientific Research.

REFERENCES

- [1] J.S. Park, "Necessity of rehabilitation and current state of domestic sewage pipe network", *KSCE J. Civ. Eng.*, vol. 55, pp. 135-143, 2007.
- [2] M. Alexander, A. Bentur, and S. Mindess, *Durability of Concrete: Design and Construction.*, CRC Press: Boca Raton, Florida, United States, 2017.
[<http://dx.doi.org/10.1201/9781315118413>]
- [3] Q.T. Phung, Effects of carbonation and calcium leaching on microstructure and transport properties of cement pastes., P.h.D. thesis, Ghent University, Belgium., 2015.
- [4] P. Zhang, F.H. Wittmann, M. Vogel, H.S. Müller, and T. Zhao, "Influence of freeze-thaw cycles on capillary absorption and chloride penetration into concrete", *Cement Concr. Res.*, vol. 100, pp. 60-67, 2017.
[<http://dx.doi.org/10.1016/j.cemconres.2017.05.018>]
- [5] J. Bao, S. Xue, P. Zhang, Z. Dai, and Y. Cui, "Coupled effects of sustained compressive loading and freeze-thaw cycles on water penetration into concrete", *Struct. Concr.*, vol. 22, no. S1, pp. 944-954, 2020.
- [6] J. Bao, S. Li, P. Zhang, S. Xue, Y. Cui, and T. Zhao, "Influence of exposure environments and moisture content on water repellency of surface impregnation of cement-based materials", *J. Mater. Res. Technol.*, vol. 9, no. 6, pp. 12115-12125, 2020.
[<http://dx.doi.org/10.1016/j.jmrt.2020.08.046>]
- [7] P. Maravelaki-Kalaitzaki, Z. Agioutantis, E. Lionakis, M. Stavroulaki, and V. Perdikatsis, "Physico-chemical and mechanical characterization of hydraulic mortars containing nano-titania for restoration applications", *Cement Concr. Compos.*, vol. 36, pp. 33-41, 2013.
[<http://dx.doi.org/10.1016/j.cemconcomp.2012.07.002>]
- [8] G. Matias, P. Faria, and I. Torres, "Lime mortars with heat treated clays and ceramic waste: A review", *Constr. Build. Mater.*, vol. 73, pp. 125-136, 2014.
[<http://dx.doi.org/10.1016/j.conbuildmat.2014.09.028>]
- [9] M. Vyšvařil, M. Pavlíková, M. Záleská, A. Pivák, T. Žižlavský, P. Rovnaníková, P. Bayer, and Z. Pavlík, "Non-hydrophobized perlite renders for repair and thermal insulation purposes: Influence of different binders on their properties and durability", *Constr. Build. Mater.*, vol. 263, p. 120617, 2020.
[<http://dx.doi.org/10.1016/j.conbuildmat.2020.120617>]
- [10] J. Bijen, *Durability of Engineering Structures Design, Repair and Maintenance.*, CRC Press: Boca Raton, Florida, United States, 2003.
- [11] P. Niewiadomski, J. Hoła, and A. Ćwirzeń, "Study on properties of

- self-compacting concrete modified with nanoparticles", *Arch. Civ. Mech. Eng.*, vol. 18, no. 3, pp. 877-886, 2018.
[<http://dx.doi.org/10.1016/j.acme.2018.01.006>]
- [12] H. Okamura, and M. Ouchi, "Self-Compacting Concrete", *J. Adv. Concr. Technol.*, vol. 1, no. 1, pp. 5-15, 2003.
[<http://dx.doi.org/10.3151/jact.1.5>]
- [13] B. Benabed, E.H. Kadri, L. Azzouz, and S. Kenai, "Properties of self-compacting mortar made with various types of sand", *Cement Concr. Compos.*, vol. 34, no. 10, pp. 1167-1173, 2012.
[<http://dx.doi.org/10.1016/j.cemconcomp.2012.07.007>]
- [14] A. Loukili, *Self-Compacting Concrete*, ISTE Ltd and John Wiley & Sons, Inc: United States, 2011.
[<http://dx.doi.org/10.1002/9781118602164>]
- [15] ACI, "Committee 237, Self-Consolidating Concrete (ACI 237R-04)",
- [16] H. Okamura, and K. Ozawa, "Mix design for self-compacting concrete", *Concrete Library of JSCE*, no. 25, pp. 107-120, 1995.
- [17] A.A. Thakare, A. Singh, V. Gupta, S. Siddique, and S. Chaudhary, "Sustainable development of self-compacting cementitious mixes using waste originated fibers: A review", *Resour. Conserv. Recycling*, vol. 168, p. 105250, 2021.
[<http://dx.doi.org/10.1016/j.resconrec.2020.105250>]
- [18] L. Antoni, L. Chandra, and D. Hardjito, "The impact of using fly ash, silica fume and calcium carbonate on the workability and compressive strength of mortar", *Procedia Eng.*, vol. 125, pp. 773-779, 2015.
[<http://dx.doi.org/10.1016/j.proeng.2015.11.132>]
- [19] H. F. W Taylor, *Cement Chemistry*, Academic Press: London, 1990, p. 475.
- [20] X. Liu, X. Lv, J. Fu, P. Peng, and G. Gai, "Application of silica fume in China", *Adv. Mat. Res.*, vol. 58, pp. 21-26, 2009.
- [21] R. Siddique, "Utilization of silica fume in concrete: Review of hardened properties", *Resour. Conserv. Recycling*, vol. 55, no. 11, pp. 923-932, 2011.
[<http://dx.doi.org/10.1016/j.resconrec.2011.06.012>]
- [22] A. Bentur, A. Goldman, and M.D. Cohen, "The contribution of the transition zone to the strength of high quality silica fume concretes", *MRS Online Proc. Lib.*, vol. 114, p. 97, 1987.
- [23] W.L. Zhong, B. Qiu, Y.H. Zhang, X. Zhao, and L.F. Fan, "Mesoscopic damage characteristics of hydrophobicity-modified geopolymer composites under freezing-thawing cycles based on CT scanning", *Compos. Struct.*, vol. 326, p. 117637, 2023.
[<http://dx.doi.org/10.1016/j.compstruct.2023.117637>]
- [24] W.L. Zhong, L.F. Fan, and Y.H. Zhang, "Experimental research on the dynamic compressive properties of lightweight slag based geopolymer", *Ceram. Int.*, vol. 48, no. 14, pp. 20426-20437, 2022.
[<http://dx.doi.org/10.1016/j.ceramint.2022.03.328>]
- [25] W.L. Zhong, Y.H. Zhang, and L.F. Fan, "High-ductile engineered geopolymer composites (EGC) prepared by calcined natural clay", *J. Build. Eng.*, vol. 63, p. 105456, 2023.
[<http://dx.doi.org/10.1016/j.jobee.2022.105456>]
- [26] W.L. Zhong, Y.H. Zhang, L.F. Fan, and P.F. Li, "Effect of PDMS content on waterproofing and mechanical properties of geopolymer composites", *Ceram. Int.*, vol. 48, no. 18, pp. 26248-26257, 2022.
[<http://dx.doi.org/10.1016/j.ceramint.2022.05.306>]
- [27] W.L. Zhong, Y.H. Sun, X. Zhao, and L.F. Fan, "Study on synthesis and water stability of geopolymer pavement base material using waste sludge", *J. Clean. Prod.*, vol. 445, p. 141331, 2024.
[<http://dx.doi.org/10.1016/j.jclepro.2024.141331>]
- [28] S.T. Kang, J.I. Choi, K.T. Koh, K.S. Lee, and B.Y. Lee, "Hybrid effects of steel fiber and microfiber on the tensile behavior of ultra-high performance concrete", *Compos. Struct.*, vol. 145, pp. 37-42, 2016.
[<http://dx.doi.org/10.1016/j.compstruct.2016.02.075>]
- [29] P. Yan, B. Chen, S. Afgan, M. Aminul Haque, M. Wu, and J. Han, "Experimental research on ductility enhancement of ultra-high performance concrete incorporation with basalt fibre, polypropylene fibre and glass fibre", *Constr. Build. Mater.*, vol. 279, p. 122489, 2021.
[<http://dx.doi.org/10.1016/j.conbuildmat.2021.122489>]
- [30] iTeh Standards, "EN 1504-3, "Products and systems for the protection and repair of concrete structures- Definitions, requirements, quality control and evaluation of conformity-Part 3: Structural and non-structural repair", Available From: https://standards.iteh.ai/catalog/standards/cen/62c5607f-c564-4802-9b11-a872dc3c4b3c/en-1504-3-2005?srsltid=AfmBOoorDs8hCwQrl_dkIlhkC7u1obgysMgD8Gjbsd0_ygJ0kMNIQexN
- [31] ANSI Webstor, "BS EN 197-1:2000, Cement. Composition, specifications and conformity criteria for common cements (British Standard)", Available From: https://webstore.ansi.org/standards/bsi/bSEN1972000?srsltid=AfmBOooxB9vFpHWMrZrStL2hh_sU99re5t56W9EnCCU7cdzi2T2LT97
- [32] iTeh Standards, "EN 13263-1 "Silica fume for concrete - Part 1: Definitions, requirements and conformity criteria", Available From: https://standards.iteh.ai/catalog/standards/cen/503d9622-7c15-4d83-95c7-c6bbdfc941a/en-13263-1-2005a1-2009?srsltid=AfmBOoqxgCBKBWq-0TEdBLZEc13M3MpAZ-9CwkO_yQwbo0CS4CyrTcG3
- [33] iTeh Standards, "EN 13263-2 "Silica fume for concrete - Part 2: Conformity evaluation", Available From: https://standards.iteh.ai/catalog/standards/cen/acecd2b0-7b30-44ed-9ce1-434a4a96a06f/en-13263-2-2005?srsltid=AfmBOor9WQuTddRQOA_9_xbpbDwjgkAPM4GHARqgKiBtr_F4uaFFCiR
- [34] EFNARC, *Guidelines for self-compacting concrete*, EFNARC: UK, 2002, pp. 1-32.
- [35] iTeh Standards, "EN 12390-5, "Testing hardened concrete-Part 5: Flexural strength of test specimens", British Standards Institution-BSI and CEN European Committee for Standardization", Available From: https://standards.iteh.ai/catalog/standards/cen/275df2f9-c466-4bb1-b41c-b8dfa9fc6d89/en-12390-5-2009?srsltid=AfmBOor-JlOIHa_tbSu44EE7-e2mqgnrquJu6je1RAHp2xvud8BlHoHr
- [36] European Standards, "EN-12504-4 Testing concrete in structures Determination of ultrasonic pulse velocity", Available From: https://www.en-standard.eu/bs-en-12504-4-2021-testing-concrete-in-structures-determination-of-ultrasonic-pulse-velocity/?srsltid=AfmBOop9fuUaMV-yjtThT6IxRRpb_0ij63MkrDlPC1-JBqNLh1G8Hwx
- [37] iTeh Standards, "EN 1015-18, "Methods of test for mortar for masonry, Part 18, Determination of water absorption coefficient due to capillary action of hardened mortar", Available From: https://standards.iteh.ai/catalog/standards/cen/d9e520b3-5f88-4368-ae91-e568d18aef5a/en-1015-18-2002?srsltid=AfmBOopHim1LDfagYHrlEazqLwBjRgGUYA0-ODfBxYzd_JhG5AKkaDJa
- [38] iTeh Standards, "12617-4 Products and systems for the protection and repair of concrete structures. Test methods Determination of shrinkage and expansion", Available From: https://standards.iteh.ai/catalog/standards/cen/dc9947b-b2ff-496d-9a3d-b8beede52589/en-12617-4-2002?srsltid=AfmBOooIqfmYyVRMnlb_rulhbUje4Q05tbGTJ2aK31-wm-ImYN-OVYH0g
- [39] ASTM, "ASTM C78, "Standard Test Method for Flexural Strength of Concrete" (Using Simple Beam with ThirdPoint Loading)", Available From: https://www.astm.org/c0078_c0078m-22.html
- [40] S. Yaseri, M. Mahdikhani, A. Jafarinoor, V. Masoomi Verki, M. Esfandiyari, and S.M. Ghiasian, "The development of new empirical apparatuses for evaluation fresh properties of self-consolidating mortar: Theoretical and experimental study", *Constr. Build. Mater.*, vol. 167, pp. 631-648, 2018.
[<http://dx.doi.org/10.1016/j.conbuildmat.2018.02.021>]
- [41] Ş. Erdoğan, C. Arslantürk, and Ş. Kurbetci, "Influence of fly ash and silica fume on the consistency retention and compressive strength of concrete subjected to prolonged agitating", *Constr. Build. Mater.*, vol. 25, no. 3, pp. 1277-1281, 2011.
[<http://dx.doi.org/10.1016/j.conbuildmat.2010.09.024>]
- [42] D. Park, S. Park, Y. Seo, and T. Noguchi, "Water absorption and

- constraint stress analysis of polymer-modified cement mortar used as a patch repair material", *Constr. Build. Mater.*, vol. 28, no. 1, pp. 819-830, 2012.
- [43] F.A. Sabet, N.A. Libre, and M. Shekarchi, "Mechanical and durability properties of self consolidating high performance concrete incorporating natural zeolite, silica fume and fly ash", *Constr. Build. Mater.*, vol. 44, pp. 175-184, 2013. [<http://dx.doi.org/10.1016/j.conbuildmat.2013.02.069>]
- [44] E. Teimortashlu, M. Dehestani, and M. Jalal, "Application of Taguchi method for compressive strength optimization of tertiary blended self-compacting mortar", *Constr. Build. Mater.*, vol. 190, pp. 1182-1191, 2018. [<http://dx.doi.org/10.1016/j.conbuildmat.2018.09.165>]
- [45] H. Salehi, and M. Mazloom, "Opposite effects of ground granulated blast-furnace slag and silica fume on the fracture behavior of self-compacting lightweight concrete", *Constr. Build. Mater.*, vol. 222, pp. 622-632, 2019. [<http://dx.doi.org/10.1016/j.conbuildmat.2019.06.183>]
- [46] A.F. Bingöl, and İ. Tohumcu, "Effects of different curing regimes on the compressive strength properties of self compacting concrete incorporating fly ash and silica fume", *Mater. Des.*, vol. 51, pp. 12-18, 2013. [<http://dx.doi.org/10.1016/j.matdes.2013.03.106>]
- [47] W. Wu, R. Wang, C. Zhu, and Q. Meng, "The effect of fly ash and silica fume on mechanical properties and durability of coral aggregate concrete", *Constr. Build. Mater.*, vol. 185, pp. 69-78, 2018. [<http://dx.doi.org/10.1016/j.conbuildmat.2018.06.097>]
- [48] X. Ma, T. He, Y. Xu, R. Yang, and Y. Sun, "Hydration reaction and compressive strength of small amount of silica fume on cement-fly ash matrix", *Construction Materials*, vol. 16, p. e00989, 2022.
- [49] G.A. Rao, "Development of strength with age of mortars containing silica fume", *Cement Concr. Res.*, vol. 31, no. 8, pp. 1141-1146, 2001. [[http://dx.doi.org/10.1016/S0008-8846\(01\)00540-3](http://dx.doi.org/10.1016/S0008-8846(01)00540-3)]
- [50] A.M. Safhi, M. Benzerzour, P. Rivard, N-E. Abriak, and I. Ennahal, "Development of self-compacting mortars based on treated marine sediments", *J. Build. Eng.*, vol. 22, pp. 252-261, 2019. [<http://dx.doi.org/10.1016/j.jobe.2018.12.024>]
- [51] A. Benli, M. Karataş, and Y. Bakir, "An experimental study of different curing regimes on the mechanical properties and sorptivity of self-compacting mortars with fly ash and silica fume", *Constr. Build. Mater.*, vol. 144, pp. 552-562, 2017. [<http://dx.doi.org/10.1016/j.conbuildmat.2017.03.228>]
- [52] V.N. Zarnaghi, A. Fouroghi-Asl, V. Nourani, and H. Ma, "On the pore structures of lightweight self-compacting concrete containing silica fume", *Constr. Build. Mater.*, vol. 193, pp. 557-564, 2018. [<http://dx.doi.org/10.1016/j.conbuildmat.2018.09.080>]
- [53] A. Alshahrani, S. Kulasegaram, and A. Kundu, "Elastic modulus of self-compacting fibre reinforced concrete: Experimental approach and multi-scale simulation", *Case Studies in Construction Materials*, vol. 18, p. e01723, 2023. [<http://dx.doi.org/10.1016/j.cscm.2022.e01723>]
- [54] M. Mazloom, A.A. Ramezaniapour, and J.J. Brooks, "Effect of silica fume on mechanical properties of high-strength concrete", *Cement Concr. Compos.*, vol. 26, no. 4, pp. 347-357, 2004. [[http://dx.doi.org/10.1016/S0958-9465\(03\)00017-9](http://dx.doi.org/10.1016/S0958-9465(03)00017-9)]
- [55] M.A. Haque, B. Chen, and S. Li, "Water-resisting performances and mechanisms of magnesium phosphate cement mortars comprising with fly-ash and silica fume", *J. Clean. Prod.*, vol. 369, p. 133347, 2022. [<http://dx.doi.org/10.1016/j.jclepro.2022.133347>]
- [56] H. Chen, Q. Chen, Y. Xu, and A.S. Lawi, "Effects of silica fume and Fly ash on properties of mortar reinforced with recycled-polypropylene", *Constr. Build. Mater.*, vol. 316, p. 125887, 2022. [<http://dx.doi.org/10.1016/j.conbuildmat.2021.125887>]
- [57] S.Y. Guo, X. Zhang, J.Z. Chen, B. Mou, H.S. Shang, P. Wang, L. Zhang, and J. Ren, "Mechanical and interface bonding properties of epoxy resin reinforced Portland cement repairing mortar", *Constr. Build. Mater.*, vol. 264, p. 120715, 2020. [<http://dx.doi.org/10.1016/j.conbuildmat.2020.120715>]
- [58] W.A. Al-Khaja, "Strength and time-dependent deformations of silica fume concrete for use in Bahrain", *Constr. Build. Mater.*, vol. 8, no. 3, pp. 169-172, 1994. [[http://dx.doi.org/10.1016/S0950-0618\(09\)90030-7](http://dx.doi.org/10.1016/S0950-0618(09)90030-7)]
- [59] C. Jiang, X. Zhou, S. Huang, and D. Chen, "Influence of polyacrylic ester and silica fume on the mechanical properties of mortar for repair application", *Adv. Mech. Eng.*, vol. 9, no. 1, pp. 1-10, 2016.
- [60] M.M. Sprinkel, Twenty-year performance of latex-modified concrete overlays. *Polymer-Modified Hydraulic-Cement Mixtures.*, ASTM International: West Conshohocken, PA, USA, 1993. [<http://dx.doi.org/10.1520/STP25552S>]
- [61] M.H.F. Medeiros, P. Helene, and S. Selmo, "Influence of EVA and acrylate polymers on some mechanical properties of cementitious repair mortars", *Constr. Build. Mater.*, vol. 23, no. 7, pp. 2527-2533, 2009. [<http://dx.doi.org/10.1016/j.conbuildmat.2009.02.021>]
- [62] A. Mallat, and A. Alliche, "Mechanical investigation of two fiber-reinforced repair mortars and the repaired system", *Constr. Build. Mater.*, vol. 25, no. 4, pp. 1587-1595, 2011. [<http://dx.doi.org/10.1016/j.conbuildmat.2010.10.017>]
- [63] A. Momayez, M.R. Ehsani, A.A. Ramezaniapour, and H. Rajaie, "Comparison of methods for evaluating bond strength between concrete substrate and repair materials", *Cement Concr. Res.*, vol. 35, no. 4, pp. 748-757, 2005. [<http://dx.doi.org/10.1016/j.cemconres.2004.05.027>]
- [64] S. Xu, Q. Ma, and J. Wang, "Combined effect of isobutyltriethoxysilane and silica fume on the performance of natural hydraulic lime-based mortars", *Constr. Build. Mater.*, vol. 162, pp. 181-191, 2018. [<http://dx.doi.org/10.1016/j.conbuildmat.2017.09.150>]